ANALYSIS OF LOCA SCENARIOS IN THE NIST RESEARCH REACTOR BEFORE AND AFTER FUEL CONVERSION

Joo Seok Baek, Lap-Yan Cheng, and David Diamond
Nuclear Science and Technology Department
Brookhaven National Laboratory, P.O. Box 5000, Upton, NY 11973-5000
jbaek@bnl.gov; cheng@bnl.gov; diamond@bnl.gov

ABSTRACT

An analysis has been done of hypothetical loss-of-coolant-accidents (LOCAs) in the research reactor (NBSR) at the National Institute of Standards and Technology (NIST). The purpose of the analysis is to determine if the peak clad temperature remains below the safety limit which is the blister temperature for the fuel. The analysis was done for two core designs, the present core with high-enriched uranium (HEU) fuel and the future converted core with the proposed low-enriched uranium (LEU) fuel.

The analysis consists of two parts. The first examines how the water would drain from the primary system following a break and the possibility for the loss of coolant from within the fuel element flow channels. The hydraulics of coolant loss is analyzed using the TRACE system thermal-hydraulic code. The second part of the analysis evaluates the fuel clad temperature separately as a function of time given that the water may have drained from many of the flow channels and the water in the vessel is in a quasi-equilibrium state. A three-dimensional heat conduction code HEATING7.3 is used in the second part of the analysis because of the limited capability of TRACE to handle non-uniform heat transfer boundary conditions. The results in all scenarios considered for both HEU and LEU fuel show that the peak clad temperature remains below the blister temperature.

KEYWORDS
NBSR, loss-of-coolant accident (LOCA) analysis, water drainage, peak clad temperature

1. INTRODUCTION

The research reactor (NBSR) at the National Institute of Standards and Technology (NIST) is a heavy water (D_2O) cooled, moderated, and reflected tank type research reactor that operates at atmospheric pressure and a design power of 20 MW. Figure 1 shows the layout of the NBSR primary system. The NBSR is cooled by forced upward flow through two concentric plena below the lower grid plate of the reactor. There are thirty fuel elements in the core that are fed by these plena. The fuel elements (see Figure 2) are split axially into two halves with a 7 in (17.8 cm) unfueled gap located between the two halves at the mid-plane. Each (upper or lower) half-element has 17 curved fuel plates and two outside plates, each fitting into two side plates. The plates define 18 flow channels as shown in Figure 2.

The licensing analysis of the loss-of-coolant accident (LOCA) in the NBSR is addressed in the Safety Analysis Report (SAR) [1]. Chapter 6 of the SAR discusses the emergency cooling system (ECS), and Chapter 13 discusses the low probability of a significant pipe break: *"the main piping is located in protected areas, system pressures are low, and flow rates are small so that wear is not an issue."* Therefore, the probability of a large break (LB), including a double-ended guillotine break (GB), is extremely low. For small breaks (SBs) where the operator has time to take action, procedures are in place

[2] to a) mitigate a loss of water by tripping pumps and closing control valves to isolate the reactor vessel after the falling water level in the vessel is detected by instrumentation, and b) assure that emergency cooling water continues to flow for as long as needed.

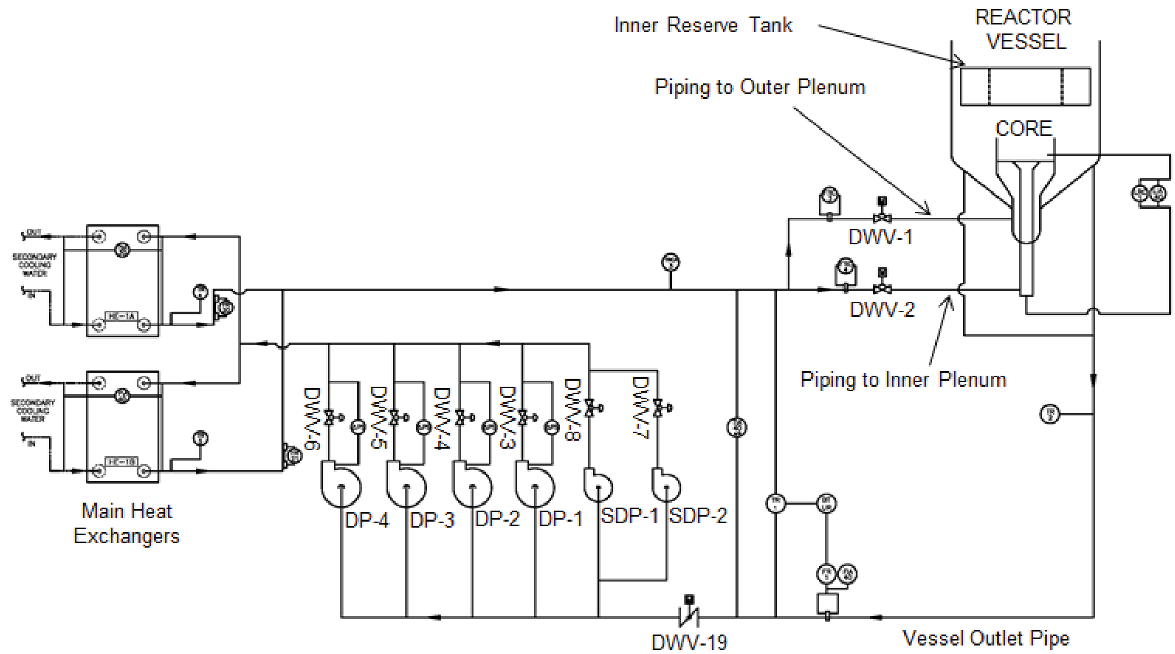

Figure 1. NBSR Primary System.

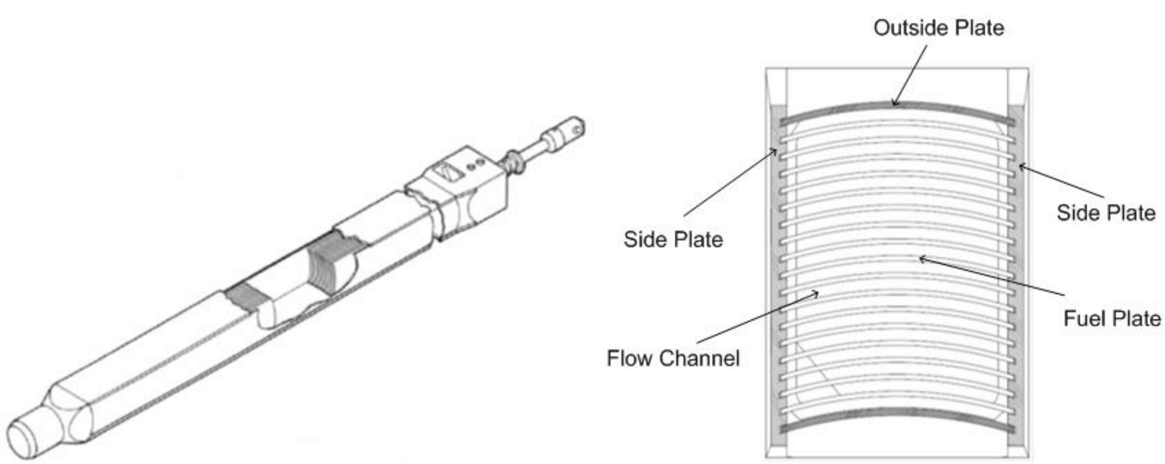

Figure 2. Cutaway Isometric Drawing and Horizontal Cross Sectional View of Fuel Element.

Chapter 13 also refers to an analysis [3] of why the ECS will provide sufficient water to cool the fuel elements (FEs) in a LOCA if all the flow channels remain filled with water. That analysis is based on assuming that the emergency water would flow due to gravity from the inner reserve tank (IRT, Component 11 in Figure 3) through the emergency cooling distribution pan (see Figure 4) above the fuel elements (the green rectangular columns in Figure 3) into all the flow channels replacing any water that boils away. In that analysis the makeup flow rate is restricted by the condition of counter-current flow limiting.

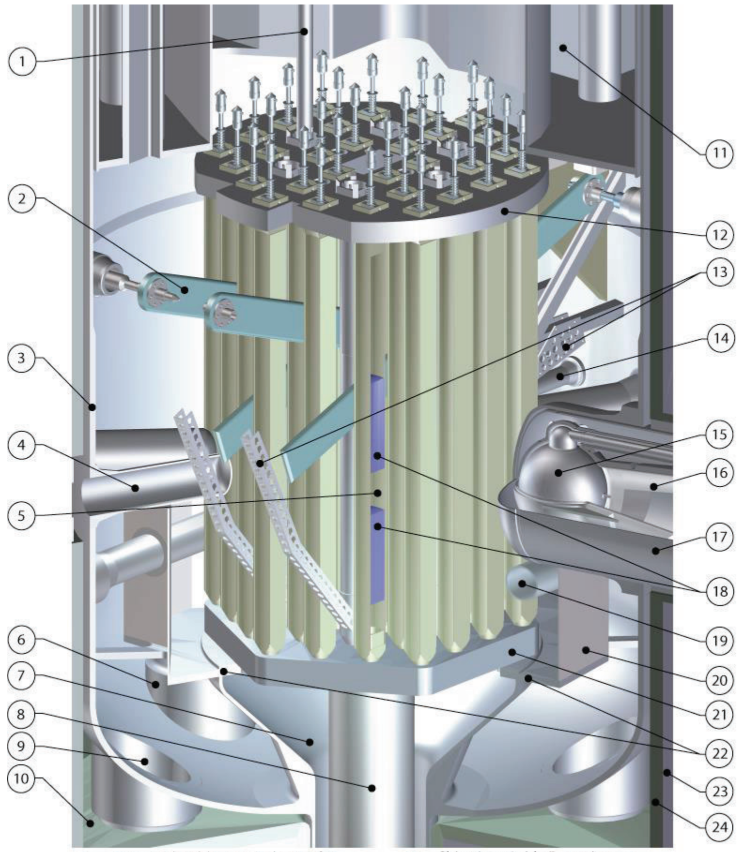

1 Poisoned Hold Down Tube (1 of 7)
2 Shim Arm #2
3 Reactor Vessel
4 BT-2 Thimble
5 Element Unfueled Gap
6 D_2O Outlet (1 of 2)
7 D_2O Inlet - Outer Plenum
8 D_2O Inlet – Inner Plenum
9 Fuel Transfer Chute Opening
10 CO_2 Filled Region
11 Inner Reserve Tank
12 Upper Grid Plate w/30 Elements
13 Shim Arm Guide Extension # 3
14 RT-3 Pneumatic Tube
15 Cold Source Moderator Chamber
16 Cold Source Insulating Vacuum
17 Cold Source D_2O Cooling Jacket
18 Fuel Plates, Upper and Lower Sections
19 Through Tube (North)
20 Heavy Water Holdup Pan
21 Lower Grid Plate
22 Outer Plenum Flange
23 Steel (Thermal Shield)
24 Lead (Thermal Shield)

Figure 3. Reactor Vessel and Internal Structures

However, until recently [4], no analysis had been done considering scenarios that lead to the draining of water from the flow channels. In these cases, the cooling on the inside of the fuel element is from the IRT water that falls (as liquid film) only along the inner surface of one of the side plates in the fuel elements; with the remaining surfaces within the fuel element exposed to gas. The reason for this configuration is demonstrated in Figure 4, which shows the situation with the water drained from the vessel above the fuel elements. On the figure it can be seen that the IRT water streams hit one side plate of the upper section of the 30 fuel elements (and seven other positions). The analysis herein discusses what would happen when this was the cooling available in scenarios where the flow channels within the fuel elements are drained.

Three locations that cover the limiting locations for pipe breaks and GB and SB break sizes considered are given in Table I (see also Figure 1) along with case numbers. Case 1 and 4 in the table are for a pipe upstream of the primary and shutdown pumps and the other cases are downstream of the pumps and take into account that the core inlet water is from two plena which feed the inner core of six fuel elements and the remaining 24 elements separately. As will be discussed below, only Cases 2 and 3 require detailed analysis for heat conduction in the fuel element with the flow channels drained.

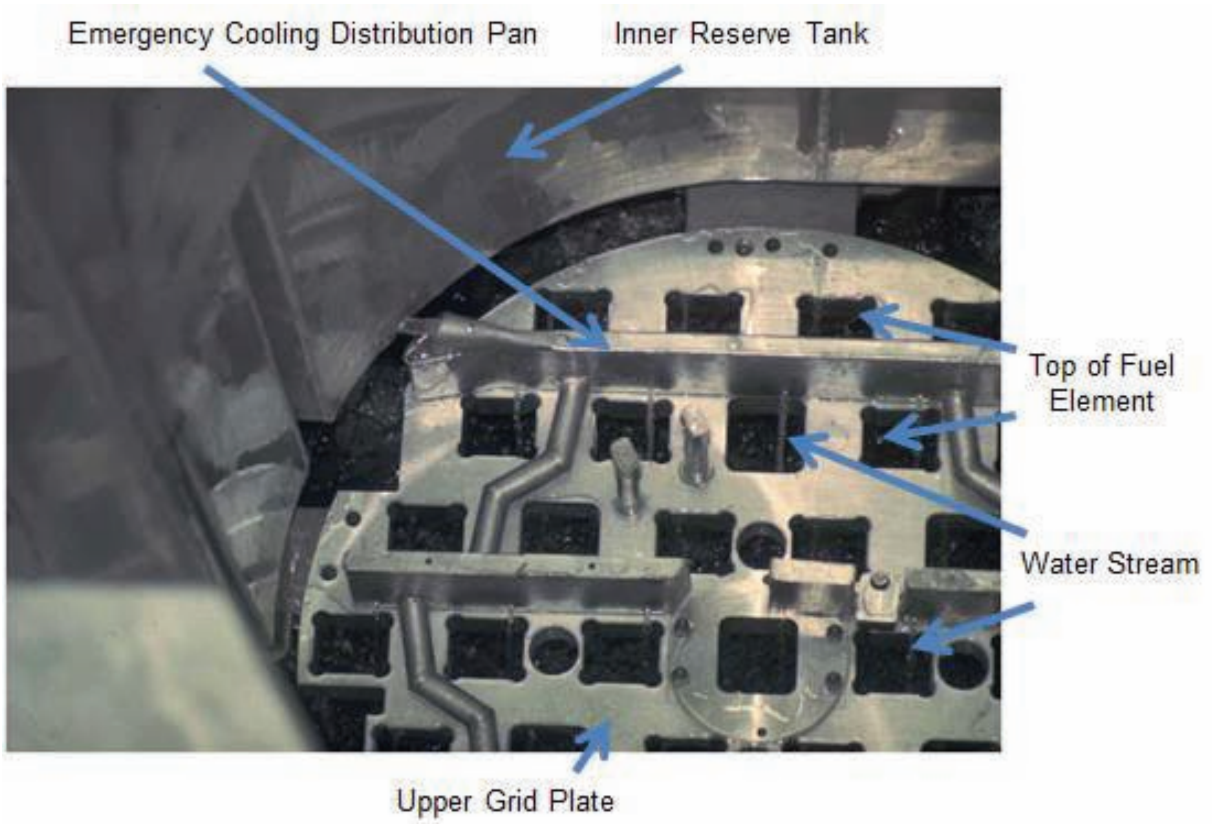

Figure 4. IRT Water Streams into Fuel Elements through Nozzles of Emergency Cooling Distribution Pan.

The analysis consists of two types of calculations. The first (see Section 2) examines how the water would drain from the primary system and how the remaining water in the vessel would reach a quasi-equilibrium condition following a break, and the potential for the loss of coolant within the fuel element flow channels. This analysis is independent of whether the fuel is high enriched uranium (HEU) or low enriched uranium (LEU) and is performed using the TRACE computer code (V 5.0 Patch 3) [5]. TRACE cannot predict open-channel liquid film flow vertically downward in a channel and doesn't have the capability to predict three-dimensional heat conduction. Hence, the second type of calculation (see Section 3) uses the three-dimensional heat conduction code HEATING7.3 [6]. In this analysis the liquid film is modeled by considering a heat transfer boundary condition for a very small portion of the fuel plate. An insulating boundary condition is assumed for the remaining part of fuel plate exposed to gas.

It should be noted that this analysis differs somewhat from that reported in Reference 4. In the previous studies the shutdown pumps (SDP-1 and SDP-2 in Figure 1) came on automatically when the primary pumps (DP-1 through DP-4 in Figure 1) trip due to low water level. However, new instrumentation is being introduced so that upon receiving a LOCA signal (low water level), the shutdown pumps will not start and the outlet valves (DWV-7 and DWV-8 in Figure 1) will not automatically open, thus eliminating a potential flow path for draining the vessel. The analysis reported on herein assumes this new mode of operation.

Table I. Break Locations and Sizes

Case No.	Location	Size / Remark
Guillotine Break		
1	18-inch pipe between the reactor vessel outlet and the control valve DWV-19	2×0.1508 m^2
2	14-inch pipe between the control valve DWV-1 and the outer plenum	2×0.089 m^2
3	10-inch pipe between the control valve DWV-2 and the inner plenum	2×0.0509 m^2
Small Break		
4	18-inch pipe between the reactor vessel outlet and the control valve DWV-19	Not simulated
5	14-inch pipe between the control valve DWV-1 and the outer plenum -	TRACE simulation only
6	10-inch pipe between the control valve DWV-2 and the inner plenum	TRACE simulation only

2. ANALYSIS OF WATER DRAINAGE

Figure 5 shows the TRACE nodal diagram for the NBSR. The NBSR model consists of the reactor vessel, primary piping from vessel outlet to inlet, upper plenum, inner reserve tank, emergency cooling distribution pan, holdup pan, primary pumps, heat exchanger, fuel elements, and flow channels. The right and left parts of the figure represent the inner core and outer core, respectively. The inner and outer cores include 6 and 24 fuel elements, respectively. The TRACE model consists of PIPE, PUMP, VALVE, FILL, and BREAK components. The nodes with red color represent the fuel plates even though they are not thermally modeled. The main objectives of the TRACE simulations are to investigate water drainage and determine the timing of the uncovering of the fuel plate. The effect of not modeling thermal source/sink is negligible.

Figure 5 also shows “VALVE” components with arrows to simulate different pipe breaks through which the coolant is discharged into the Process Room. LOCAs are simulated by opening these valve components and, if necessary, closing the valves connecting the two adjacent pipes to model guillotine breaks. VALVE-51 and VALVE-70 are also separately used to represent the actual DWV-1 and DWV-2 valves at the NBSR in the SBLOCA simulations.

2.1. Guillotine Break LOCAs

In a GBLOCA the water level in the upper plenum drops rapidly from its normal operating level of 4.04 m (159 in) as the coolant is discharged from the vessel through the break. When the level reaches 3.56 m (140 in), a LOCA signal is generated along with the trip of the primary coolant pumps. The primary pump discharge valves (DWV-3 through DWV-6 in Figure 1) are completely closed 3 s after the LOCA signal. Procedures are in place for the operator to close control valves DWV-1, DWV-2, and DWV-19 after a LOCA signal; however, it is assumed that this cannot happen in the time frame of interest for a GBLOCA. Reactor trip occurs due to a trip signal caused by low flow in the primary system or LOCA signal (low water level). The water level reaches the elevation of the top of the fuel elements as the coolant continues being discharged. The vessel water level decreases further while the water level inside the fuel elements stays at their top elevation in Case 1 (because of the closure of valves downstream of the pumps). However, in Cases 2 and 3, the inside of the fuel elements are completely drained while the vessel water level stays at the top elevation of the fuel elements. In the TRACE model, GBLOCAs are simulated by closing VALVE-102 and opening VALVE-3 and VALVE-22 (Case 1), closing VALVE-51 and opening VALVE-1 and VALVE-2 (Case 2), and closing VALVE-70 and opening VALVE-23 and VALVE-32 (Case 3). Table II shows the sequence of important events after these guillotine breaks and the collapsed water levels inside the vessel and flow channels in the upper section are depicted in Figure 6.

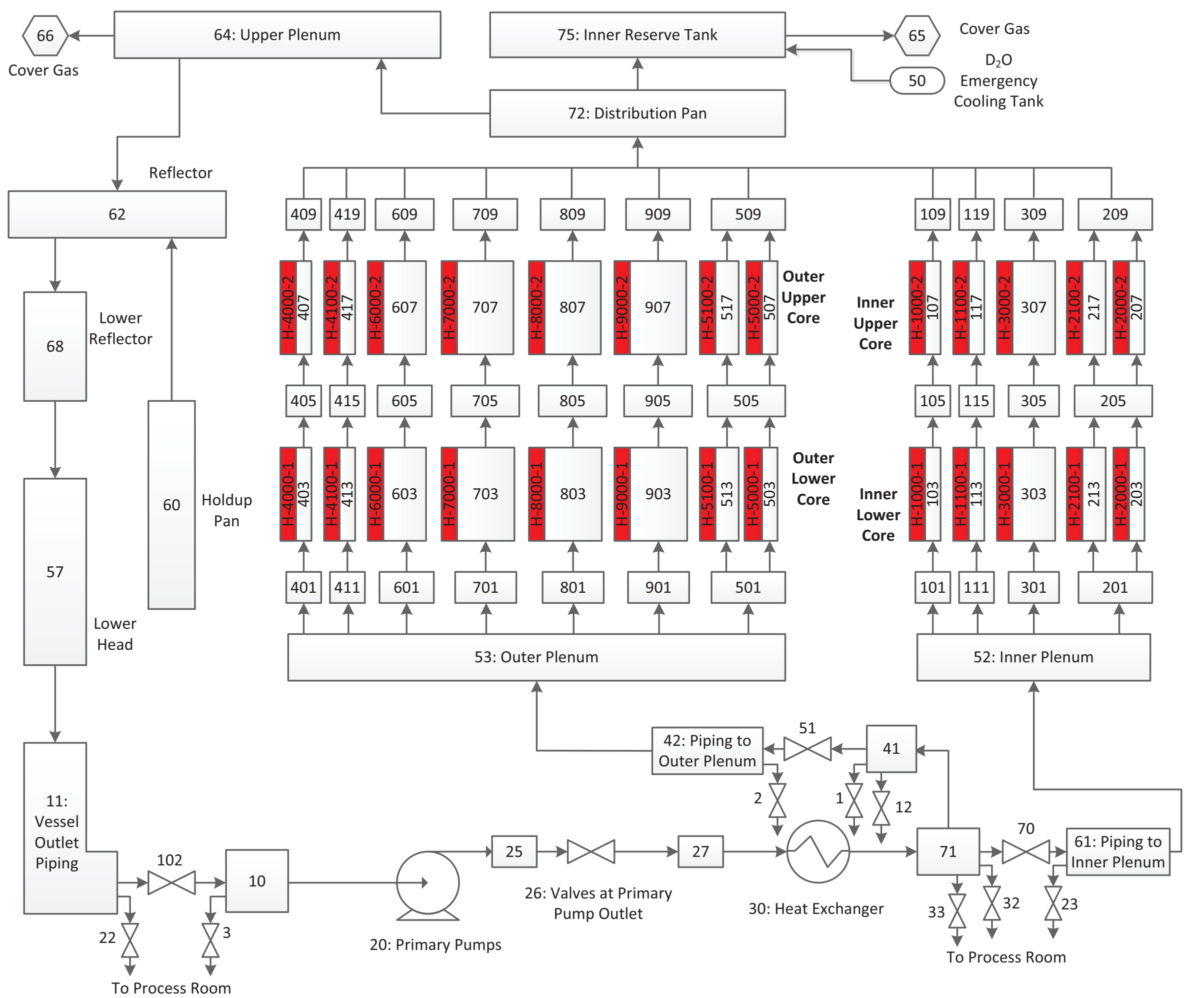

Figure 5. Nodal Diagram of TRACE Model for NBSR.

Table II. Sequence of Events after Guillotine Breaks

Event	Time (s)		
	Case 1	Case 2	Case 3
• Guillotine break occurs at different location for each case. • Water level drops in the upper plenum. • Water flows into the vessel from the IRT via the distribution pan	0.0	0.0	0.0
• Flowrate at the vessel outlet pipe decreases to the setpoint of low outer primary flow (≤4,700 gpm): Case 1. • Flowrate at the inner plenum inlet pipe decreases to the setpoint of low inner plenum flow (≤1,200 gpm): Case 2. • Flowrate at the outer plenum inlet pipe decreases to the setpoint of low outer plenum flow (≤4,700 gpm): Case 3.	2.5	0.4	0.4
• First reactor scram signal is generated due to low level: Case 1. • First reactor scram signal is generated due to low inner plenum flow: Case 2. • First reactor scram signal is generated due to low outer plenum flow: Case 3.	2.6	0.8	0.8
• LOCA signal is generated due to low level (≤3.56 m). • Main coolant pumps are tripped.	2.6	1.5	2.2
• Valves at the main coolant pumps outlets are completely closed.	5.6	4.5	5.2
• Water level outside the fuel elements reaches the elevation of the top of the upper fuel plate.	9.4	NA	NA
• The fuel plate in the upper section of the FE (Node-407) starts to be uncovered.	NA	8.6	12.7
• The fuel plate in the upper section of the FE (Node-407) is completely uncovered.	NA	~12.3	~15.6
• Water level outside the fuel element reaches the elevation of the bottom of the upper fuel plate.	~10.9	NA	NA
• Simulation ends.	30.0	30.0	30.0

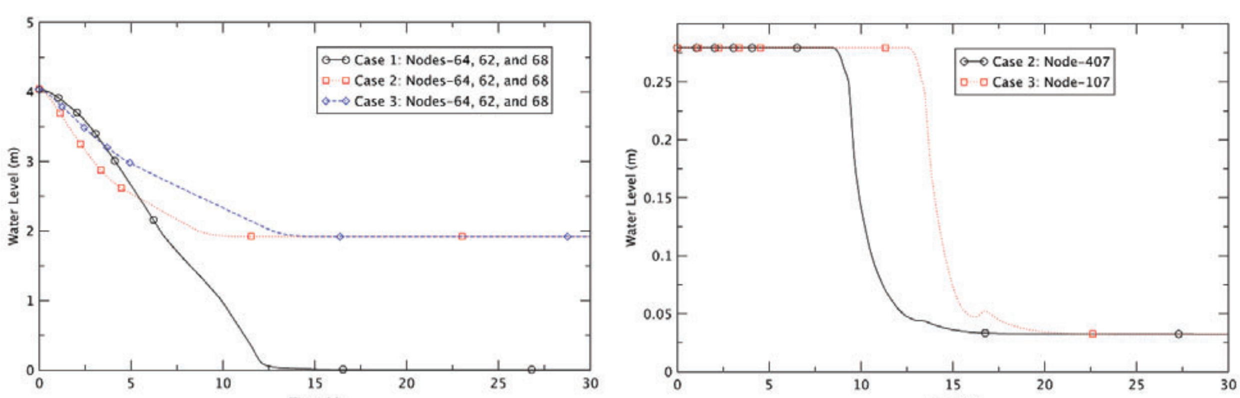

Figure 6. Water Levels inside Vessel (Left) and Upper Section of Fuel Element (Right).

The water distribution in the NBSR vessel is shown in Figure 7 for the quasi-equilibrium end-state. The grey color indicates the available heavy water. In Case 1 the outside surface of upper sections of the fuel elements are exposed to gas, which might be helium or air. The Helium Sweep Gas System supplies additional gas when the pressure drops due to the break and there is the possibility of air entering through the break. Because the end fittings of the fuel elements and any other tubes inserted into the lower grid plate are conical, leakage of water down through the fuel element seats is not expected [1] and Figure 7 shows the outside of the fuel elements submerged in the water of the hold-up pan. Therefore, since the flow from the IRT will replenish any losses inside the elements resulting from boiling, there is adequate cooling to keep the clad temperatures low and there is no need to do analysis with HEATING7.3 in Case 1. In Cases 2 and 3, however, if the operator actions to close the control valves in the primary system are not taken for at least 15 seconds after the LOCA signal, the coolant will drain from the fuel elements (FEs) while the outside of FEs are in contact with water. The water coming from the IRT (Figure 4) forms a liquid film on the inside surface of one side plate in Cases 2 and 3.

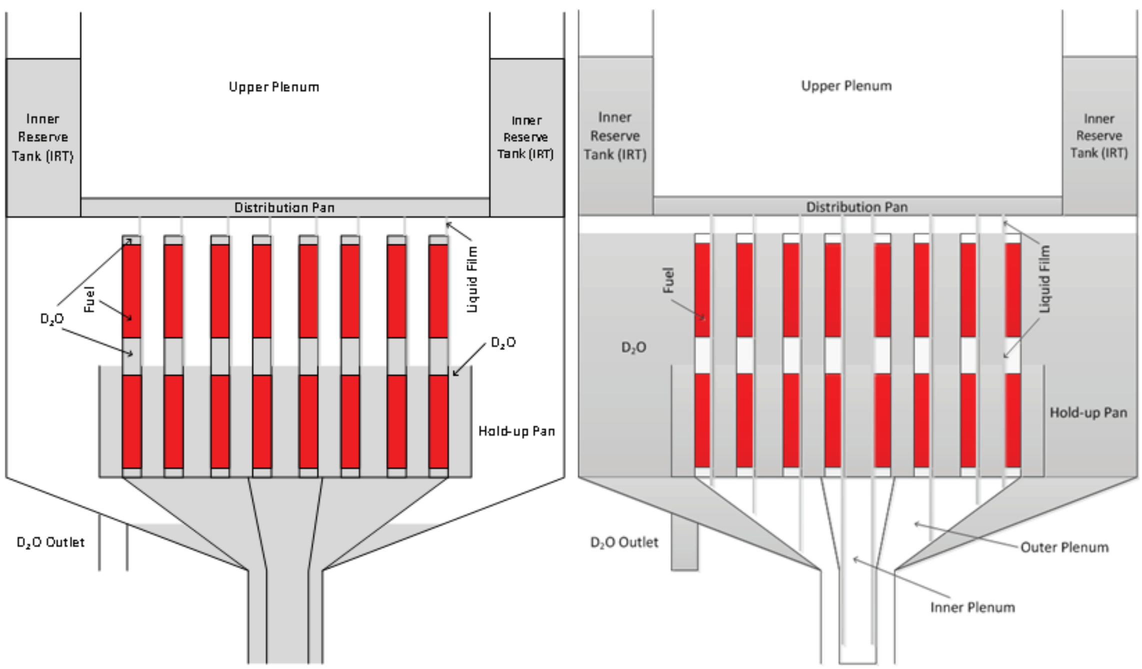

Figure 7. End-state of Coolant after GBLOCA in Case 1 (Left) and Cases 2 and 3 (Right).

2.2. Small Break LOCAs

One difference between an SBLOCA and a GBLOCA is that the operator has time to take action. For the case with the break at the vessel outlet (Case 4) this makes no difference and the sequence of events proceeds as in the case with the GBLOCA (Case 1) except at a much slower rate. The end-state for the SBLOCA at the outlet pipe is the one in Case 1 as shown on the left-hand side of Figure 7. As stated for Case 1, there is adequate cooling to keep the clad temperatures low and there is no need to do analysis with HEATING7.3. This is particularly true for this case since the reduction of vessel water level occurs much later than in the GBLOCA case and hence, decay heat levels are much lower.

The simulations have some similarity to the GBLOCA Cases 2 and 3 in that because of the tripping of the primary pumps and the closure of the valve in their discharge lines, the water in the vessel outside of the fuel elements cannot drain. However, in these cases the slow evolution of the event means that operator actions can be effective. The operator shuts the control valves (DWV-1, DWV-2, and DWV-19) in the primary system and therefore, the water in the fuel elements fed by the inner plenum cannot drain when the break is at the outer plenum and similarly, the elements fed by the outer plenum cannot drain when the break is at the inner plenum.

The results are also used to see how much time it would take to drain the fuel elements in Cases 5 and 6. The results [4] for the 6.8 cm^2 break show that in these cases the water level reaches the top of the fuel plates in ~1700 s. The fuel plates in either the top or bottom of the element take 5-18 seconds to drain depending on the break location. Larger breaks will of course drain sooner and smaller breaks later. Later uncovering of the fuel elements in SBLOCAs results in much lower decay power. Therefore, the peak clad temperature (PCT) analysis using HEATING7.3 is not performed for Cases 5 and 6 because the consequences of those cases are bounded by the results for the GBLOCAs.

3. ANALYSIS OF PEAK CLAD TEMPERATURES

If forced flow (delivered by the primary pumps) becomes unavailable after a LOCA and the fuel elements drain, as predicted by TRACE, the decay heat will be transferred to the water from the IRT falling as a film on one of the side plates inside fuel elements and to the surrounding quiescent coolant outside the fuel elements. The latter heat transfer is by natural convection, and nucleate boiling if the surface temperature is high enough. The clad and fuel temperatures may rise depending upon the decay power and the availability of the coolant. A condition for maintaining the integrity of the fuel cladding is that the cladding remains below its blistering temperature, 450°C for HEU [1] and 380°C for LEU (preliminary). A recent study [4] showed that the cooling from the liquid film alone was adequate to keep the HEU fuel clad temperature below the minimum blister temperature even without the surrounding coolant outside the fuel element. However, as a result of its lower blister temperature the falling film alone was not clearly adequate for the proposed LEU fuel. The current analysis is to determine the clad temperature for both HEU and LEU fuel when the flow channels within the fuel elements are drained and the elements are surrounded by heavy water.

3.1. Modeling of Heat Conduction

As shown in Figure 2, the 18 flow channels inside a fuel element are defined by the 17 fuel plates, two outside plates, and two side plates. In the HEATING7.3 simulations nine fuel plates, one outside plate, and halves of the two side plates are taken into consideration as shown in Figure 8 for LEU fuel. In Figure 8, the numbers after “R” indicate “Region” numbers of the model. Detailed information about modeling the HEU fuel is available in Reference 4 and References 7 and 8 present the dimensions and materials of the LEU fuel. The height of the fuel plate for both fuels is 33.02 cm (in Z-direction) and the fueled region is from 1.27 cm to 29.21 cm (in Z-direction) in the upper section. The outside dimensions of the HEU and LEU fuels are identical. The average thickness of fuel meat of the latter is much thinner (0.0215 cm) than the former (0.0508 cm) with the LEU fuel meat being a U10Mo alloy and the HEU fuel meat U_3O_8 in an aluminum powder dispersion. A zirconium interlayer which is expected to be 0.00254 cm thick exists between the fuel meat and clad of the LEU fuel. The region numbers of the zirconium interlayers are not presented in Figure 8. The materials of the clad and outside plate are the same (Aluminum alloy 6061 O) and the material of the side plate is Aluminum alloy 6061 T6 for both HEU and LEU fuels. The number of mesh points in the X, Y, and Z directions are 40, 135 and 53, respectively.

3.2. Modeling of Liquid Film and Heat Transfer to Liquid

The largest possible mass flowrate from the IRT is 2.8 kg/s ($\dot{m}_{IRT}$) when the water level in the vessel is lower than the bottom elevation of the IRT. The distribution pan distributes this flow as shown in Figure 4. By design the emerging jet will hit the inside of the upper end adapter of each fuel element forming a liquid film and continue to flow down one of the side plates. When the liquid film reaches the section where the fuel plates begin, it is first assumed that the water in the liquid film will distribute evenly among the 18 flow channels. The liquid film mass flowrate in each of the 18 flow channels in each fuel element is then 4.2 g/s. The water flowing down each channel is in contact with three walls, a side plate and two fuel plates (or a fuel plate and an outside plate). Assuming downward channel flow, the film thickness (measured from the inside surface of the side plate) is calculated by a force balance between the gravitational force and wall shear [4]. The friction coefficient for the wall shear can be evaluated using the Blasius equation for open channel flow presented by Yen [9]. Reference 4 discusses how the film thickness is calculated to be 0.12 cm with the concept of open channel flow when film mass flowrate is 4.2 g/s in a flow channel.

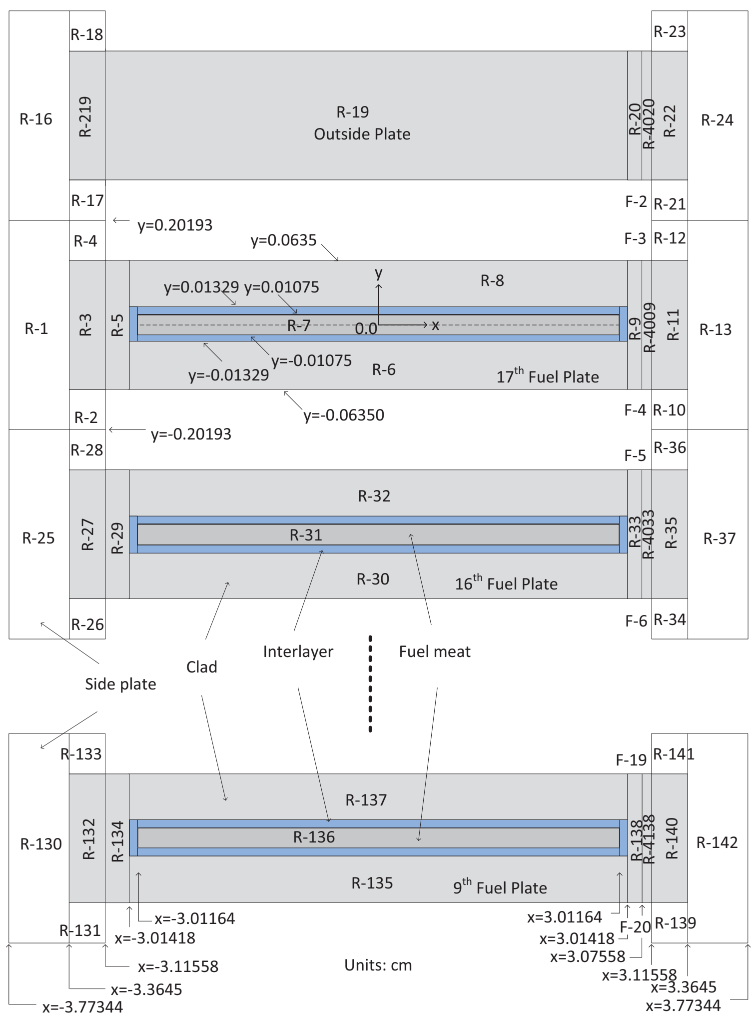

Figure 8. Regions of Nine Fuel Plates, Side Plates and Outside Plate of LEU in X-Y Plane (not to scale)

In Figure 8 the total length of R-9 and R-4009 of the 17^{th} plate is about 0.1 cm in the X-direction. This is consistent with a film thickness of 0.1 cm, conservatively chosen as the base film thickness. The falling liquid film is simulated by applying a boundary condition (heat transfer coefficient). It is to the outer surfaces of R-9 and R-4009 (facing the Y-direction), and R-10 and R-12 (facing the X-direction) while the other outer surfaces of the fuel plate and side plate are assumed to be insulated. The same method is applied to the other fuel plates.

The Wilke correlation [10], shown in Eq. (1) for turbulent subcooled film flow, is used to calculate the heat transfer coefficient (HTC) of the falling film on the inside of one side plate.

$$h\left(\frac{\mu^2}{k^3\rho^2 g}\right)^{\frac{1}{3}} = 0.0087\left(\frac{4\Gamma}{\mu}\right)^{0.4}\left(\frac{c\mu}{k}\right)^{0.34} \tag{1}$$

where, μ, k, ρ, g, Γ, and c represent the dynamic viscosity, thermal conductivity, density, gravitational acceleration, mass flowrate per length, and specific heat, respectively, of the fluid. The evaluated HTC is 0.7041 W/cm^2-°C with the film mass flowrate of 4.2 g/s per flow channel. It should be noted that the HTC of 0.7041 W/cm^2-°C is conservatively applied to all surfaces contacting the liquid film. The HTC increases as liquid temperature increases and it was observed in a sensitivity study that the contacting surface temperature rarely becomes high enough for nucleate boiling to occur. It is also conservatively assumed that heat is not transferred from the plates to gas regions of the flow channels.

Heat is also transferred from the fuel plate to the quiescent water on the outside of the fuel element. Boundary conditions are applied to the outer surfaces of the side plates using a heat flux. (The outer surface of the outside plate is conservatively assumed to have an adiabatic boundary condition.) The heat transfer coefficients are first evaluated using the Churchill and Chu correlation [11] which is appropriate for natural convection from a vertical surface and the Gorenflo correlation [12] for nucleate boiling. The former and latter correlations depend upon the difference between the surface temperature (T_s) and the surrounding water temperature (T_b) and the difference between the surface temperature and the liquid saturation temperature (T_{sat}), respectively. Heat flux from the surface of the side plate is calculated using the heat transfer coefficients and the temperature differences. The "combined heat flux" that is used is the larger of that due to natural convection or nucleate boiling.

In the HEATING7.3 simulations the boundary temperature is 41°C (temperature of water film) but 0°C is used for convenience. So nucleate boiling is assumed to occur when the predicted temperature of the side plate surface reaches the boiling temperature, i.e. a calculated temperature of 60°C (=101°C - 41°C). In the analysis the heat flux becomes zero when the surface temperature is 83.6°C. This implies reaching boiling crisis with a critical heat flux of q''_{CHF} = 132.2 W/cm^2 and a surface temperature of 83.5°C. Reference 13 presents experimental results for the critical heat flux (~130 W/cm^2) on a vertical plate with water.

3.3. Fuel Plate Power

The fuel element modeled is that with the hottest plate in the core at end-of-cycle (EOC) when decay heat is expected to be largest (and closest to the infinite irradiation condition utilized in obtaining decay power). Approximately 50% of the decay power is due to alpha and beta radiation; assumed to deposit locally at the site of origin. Hence, the steady-state power distribution is used to determine the energy deposition due to alpha and beta decay. Since calculations of gamma transport using a Monte Carlo method were available for HEU [14], the distribution of gamma energy deposition in the fuel meat, clad, and other parts of the fuel element was explicitly taken into account. The gamma energy deposition distribution for LEU is assumed to be the same as the one for HEU.

The decay power fraction used in the analysis for the fuel at end-of-cycle is from the decay heat model in RELAP5 [15]. It is assumed that decay power is removed without problem until the fuel element starts to drain. Hence, the HEATING7.3 calculation uses an initial decay heat corresponding to the time that TRACE calculates the water level reaching the top of the coolant channels.

3.4. Steady-State Conditions

Transient runs begin when the upper fuel plates have been uncovered and it is assumed that the temperatures in the fuel element have not changed from normal operating conditions. To obtain the steady state temperatures, HEATING7.3 has been run with a heat transfer coefficient (as a boundary condition) commensurate with the flowrate in a flow channel under normal operating conditions. The heat transfer coefficient of 2.0 W/cm^2-°C is applied to all outer surfaces of the mesh regions (Figure 8). The hot spot is located in the bottom of the 17th fuel plate (the one next to the outside plate) in the upper section. Reactor inlet and outlet temperatures are 38°C and 46°C, respectively, during normal operation [1]. The steady-state average temperatures are compatible with the steady-state results predicted by RELAP5 for non-LOCA analyses [7,8].

3.5. Clad Temperature after GBLOCA

The GBLOCA quasi-equilibrium end-state of Figure 7 (Cases 2 and 3) is considered for the HEATING7.3 simulations. The flow channels have been drained and the outside of the fuel elements are submerged in the water that has not drained from the vessel. Two cases are considered with different assumptions about the mass flowrate of the falling liquid film.

As discussed in Reference 4 the thickness of the falling liquid film on the inside of one side plate depends on the coolant mass flowrate and its thermal properties and is expected to be 0.12 cm if the flow is uniformly distributed across the side plate. Analysis has been conducted with a film thickness of 0.1 cm to conservatively represent the actual thickness (and with a thinner film as will be explained below).

The results for the peak clad temperature (relative to a reference temperature) in the upper fuel section are shown in Figure 9. The ordinate represents the temperature difference between the clad surface and the falling liquid film and the abscissa is the time after the fuel plate is uncovered (it occurs 7.8 s after reactor scram as shown in Table II but conservatively assumed to occur 7 s after reactor trip). The clad temperatures start increasing rapidly from time zero because the power is higher than the cooling capacity of the liquid film and the quiescent water outside the fuel elements and the rate of the temperature increase becomes smaller as the decay power decreases. The maximum temperature difference is 171°C at 23 s for the HEU fuel and 187°C at 25 s for the LEU fuel. These peak temperatures occur toward the bottom of the 17th (end) fuel plate where the decay heat is highest. The reason for the higher temperature with the LEU fuel is that it has slightly higher power than the HEU fuel in the 17th fuel plate.

In the above simulations, it was assumed that the water is evenly distributed among the 18 coolant flow channels in a fuel element and the film thickness in each flow channel is evaluated to be 0.12 cm. Figure 4 shows the water supply from the IRT to the 30 fuel elements and seven other positions after the vessel water level becomes lower than the top elevation of the fuel elements. As shown in the figure, the water coming from the nozzles of the distribution pan is skewed to one side (not the center) of the upper portion of the fuel element. The distribution of water into flow channels would be influenced by where the water jet impinges and the presence of internal structures (the center metal bar, latch bars, and windows on the side plates near the water impingement point) that interrupt the spread of the liquid film. Based on Figure 4, the distribution would be skewed to one side of the side plate. Hence, the film thickness in the flow channels based on uniform flow distribution is only an approximation.

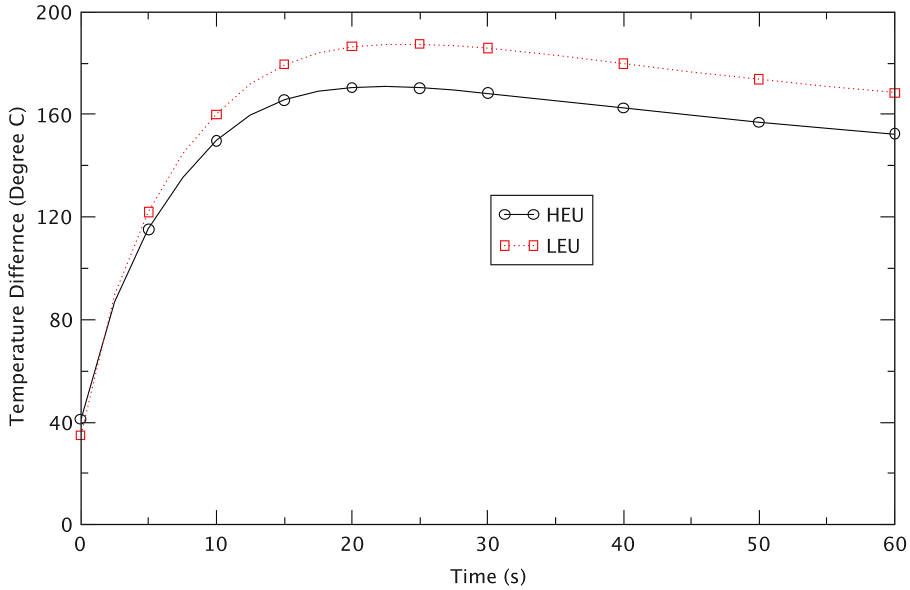

Figure 9. Peak Clad Temperature with Uniform Film Thickness (0.1 cm) after GBLOCA

In the following it is assumed that the film mass flowrate is considerably smaller along one side of the side plate and that the nine fuel plates modeled in HEATING7.3 are located on the side away from where the water impinges (note that the fuel plates are running parallel to the emerging jet from the distribution pan). A liquid film mass flowrate of only one-fifth (0.84 g/s per fuel channel) of the average film flowrate is considered. The heat transfer coefficient of the film is evaluated to be 0.370 W/cm^2-K at 0.84 g/s using Eq. (1). The film thickness is evaluated to be 0.052 cm but conservatively assumed to be 0.04 cm.

However, if a very thin film is assumed along the right side, it must be recognized that there is a significant amount of water dripping down vertically from the center bar that is part of the fuel element structure above the height where the fuel plates are located. Water behavior after entry into a fuel element was observed in mockup tests with the upper part of a fuel element and leads to the assumption that due to the center bar there is a film flowing with a flowrate of about one-fourth of the total flow (0.7 kg/s = 1/4 of 2.8 kg/s) which conservatively covers half of the central fuel plate no. 9 (the mesh region R-135 in Figure 8) from 0.0 cm to 3.2 cm in the X-direction. For this liquid film, the heat transfer coefficient is evaluated to be 0.494 W/cm^2-K using the Wilke correlation for turbulent subcooled film flow.

Figure 10 shows that the effect of reducing the film thickness and adding cooling to a portion of plate no. 9 is to increase the peak clad temperature difference by ~10ºC. The maximum temperature difference becomes 180ºC at 25 s for the HEU fuel and 196ºC at 25 s for the LEU fuel. If the film temperature is assumed to be 101°C (the saturation temperature of D_2O at atmospheric pressure), the maximum temperatures of the HEU and LEU fuels become 281ºC and 297ºC, respectively, and are lower than their blister temperatures (450°C for HEU and 380°C for LEU). Additionally, there are eight more fuel plates plus another outside plate that are present but not modeled in HEATING7.3 and they are cooled more effectively because more water is available for them than for the plates being modeled in the simulation. This fact will lead to a lower PCT than calculated and shown in Figure 10. Hence, again it can be concluded that the GBLOCA scenarios will not lead to any fuel damage.

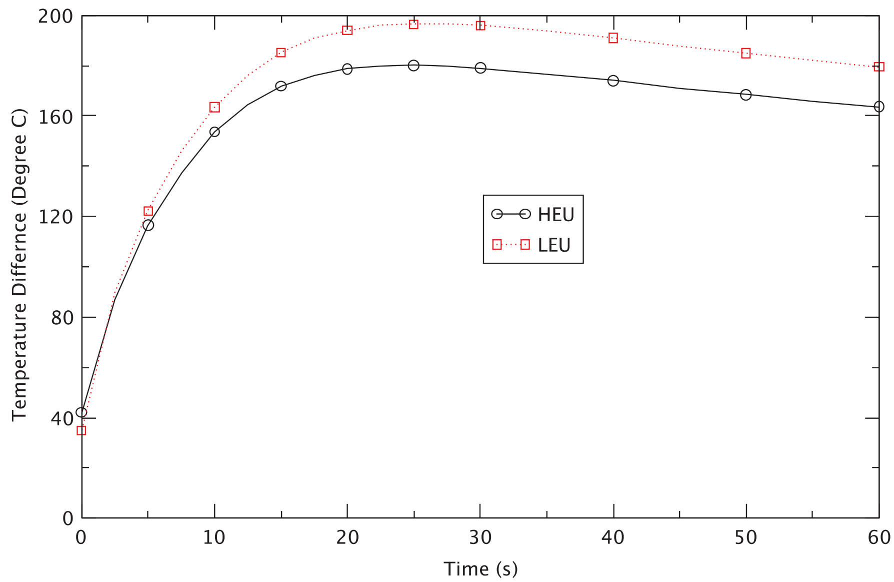

Figure 10. PCT with Reduced Film (0.04 cm) on Side Plate and Partial Cooling of 9th Plate

4. CONCLUSIONS

Guillotine break LOCAs and small break LOCAs were considered at three different limiting break locations: (1) the 18-inch pipe at the vessel outlet; (2) the 14-inch pipe at the inlet through the outer plenum; and (3) the 10-inch pipe at the inlet through the inner plenum. TRACE has been run to investigate the hydrodynamic behavior, especially the water level inside and outside the fuel elements. For the break at the vessel outlet, because the primary pump valves close after a low level signal, the fuel elements do not drain. Cooling is through heat transfer to the coolant inside the flow channels with relatively large heat transfer area and this will continue indefinitely as emergency water is supplied by the inner reserve tank. Hence, no fuel damage is expected for either GBLOCAs or SBLOCAs at the vessel outlet.

For GBLOCAs at the inlet pipe to either the inner or outer plenums, coolant in all fuel elements will drain but vessel water will remain to cool the outside of the elements. HEATING7.3 has been used to examine the clad temperature in the fuel plates of the hottest fuel element given some coolant is available after the fuel elements have drained in a GBLOCA. The coolant available is from the inner reserve tank and the quiescent water outside the elements. The results show that the peak clad temperature will remain well below the safety limit, which is the threshold for blistering, for either HEU or LEU fuel, and hence, fuel integrity can be assured.

The corresponding situation for a SBLOCA at either the inner or outer plenums is to have water surrounding the outside of the fuel elements but only some fuel elements are drained. The fuel elements in the inner (outer) core are drained when the break is at the inner (outer) plenum. The reason that not all fuel elements are drained as in the GBLOCA is the operator actions that close the control valves that preclude the inner or outer plenum from draining. A smaller break in SBLOCA results in longer drain time and a lower decay heat level than the corresponding case of GBLOCA. Fuel integrity was shown to be maintained for the GBLOCA, and by extension, it can also be assured for these less severe SBLOCA scenarios.

ACKNOWLEDGMENTS

This work was supported by the National Nuclear Security Administration and the NIST Center for Neutron Research (NCNR). The authors appreciate the information obtained from, and the review by, Sean O'Kelly, Paul Brand, Robert Williams, and Michael Rowe at the NCNR.

REFERENCES

1. NIST, "Safety Analysis Report (SAR) for License Renewal for the National Institute of Standards and Technology Reactor - NBSR; NBSR 14, Rev 4" National Institute of Standards and Technology (NIST), Gaithersburg, MD, USA (2010).
2. NIST, "NBSR Annunciator Procedures," National Institute of Standards and Technology (NIST), Gaithersburg, MD, USA (2011).
3. L. Cheng, A. Hanson, D. Diamond, J. Xu, J. Carew, and D. Rorer, "Physics and Safety Analysis for the NIST Research Reactor," BNL-NIST-0803, Rev. 1, Brookhaven National Laboratory, Upton, NY, USA (2004).
4. J. S. Baek, L.-Y. Cheng, and D. J. Diamond, "Analysis of Loss-of-Coolant Accidents in the NBSR," BNL-105287-2014-IR, Brookhaven National Laboratory, Upton, NY, USA (2014).
5. NRC, "TRACE V5.0 Theory Manual," U.S. Nuclear Regulatory Commission, USA (2010).
6. ORNL, "Multidimensional, Finite-Difference Heat Conduction Analysis Code System, Versions 7.2i and 7.3," RSICC Code Package PSR-199, Oak Ridge National Laboratory, Oak ridge, TN, USA (2007).
7. J.S. Baek, A. Cuadra, L.-Y. Cheng, A.L. Hanson, N.R. Brown, D.J. Diamond, "Analysis of Reactivity Insertion Accident for the NIST Research Reactor Before and After Fuel Conversion," *Nuclear Technology*, **185**(1), pp. 1-20 (2014)
8. J.S. Baek, A. Cuadra, L.-Y. Cheng, A.L. Hanson, N.R. Brown, D.J. Diamond, "Analysis of Loss-Of-Flow Accident for the NIST Research Reactor with Fuel Conversion from HEU to LEU," *Nuclear Technology*, **189**(1), pp. 71-86 (2015)
9. B. C. Yen, "Open Channel Flow Resistance," *Journal of Hydraulic Engineering*, pp. 20 – 39, January (2002)
10. Wolverine Tube Inc., "Wolverine Engineering Data Book II," Chapter 5 (2001).
11. F. P. Incropera, and D.P. DeWitt, *Fundamentals of Heat and Mass Transfer*, Fourth Edition, Chapter 9.6, John Wiley and Son, (1996).
12. Wolverine Tube Inc., "Wolverine Engineering Data Book III," Chapter 9 (2006).
13. A. Mourgues, V. Hourtane, T. Muller, and M. Caron-Charles, "Boiling Behavior and Critical Heat Flux on a Horizontal and Vertical Plate in Saturated Pool Boiling with and without ZnO Nanofluid," *International Journal of Heat and Mass Transfer*, **Vol. 57**, pp. 595 – 607 (2013).
14. R. Williams, "Gamma Ray Heating in Fuel Element L-3," and "Heat Distribution in LOCA Calculations - Continued," Unpublished results, NIST Center for Neutron Research (2014).
15. ISL, "RELAP5/MOD3.3 Code Manual," NUREG/CR-5535/Rev1, Information Systems Laboratories, Inc., Rockville, MD and Idaho Falls, ID, USA (2001).